Human Molecular Genetics, 2015, Vol. 24, No. 24 6921–6931

doi: 10.1093/hmg/ddv396
Advance Access Publication Date: 26 September 2015
Original Article

ORIGINAL ARTICLE

Targeting estrogen receptor β as preventive therapeutic strategy for Leber's hereditary optic neuropathy

Annalinda Pisano[1], Carmela Preziuso[1], Luisa Iommarini[4], Elena Perli[1], Paola Grazioli[2], Antonio F. Campese[2], Alessandra Maresca[5,6], Monica Montopoli[7], Laura Masuelli[3], Alfredo A. Sadun[8], Giulia d'Amati[1], Valerio Carelli[5,6], Anna Ghelli[4,*] and Carla Giordano[1,*]

[1]Department of Radiological, Oncological and Pathological Sciences, [2]Department of Molecular Medicine, [3]Department of Experimental Medicine, Sapienza University of Rome, Rome, Italy, [4]Department of Pharmacy and Biotechnology (FABIT), [5]Neurology Unit, Department of Biomedical and NeuroMotor Sciences (DIBINEM), University of Bologna, Bologna, Italy, [6]IRCCS Institute of Neurologic Science of Bologna, Bellaria Hospital, Bologna, Italy, [7]Department of Pharmacology and Anesthesiology, University of Padua, Padua, Italy and [8]Doheny Eye Institute, University of California Los Angeles, Los Angeles, USA

*To whom correspondence should be addressed at: Department of Radiological, Oncological and Pathological Sciences, Sapienza University of Rome, Policlinico Umberto I, Viale Regina Elena 324, 00161 Rome, Italy. Tel: +39 0649973331; Fax: +39 064461484; Email: carla.giordano@uniroma1.it (C.G.); Department of Pharmacy and Biotechnology (FABIT), University of Bologna, Via Irnerio 42, Bologna, Bologna, Italy. Tel: +39-0512091282; Fax: +39-051242576; Email: annamaria.ghelli@unibo.it (A.G.)

Abstract

Leber's hereditary optic neuropathy (LHON) is a maternally inherited blinding disease characterized by degeneration of retinal ganglion cells (RGCs) and consequent optic nerve atrophy. Peculiar features of LHON are incomplete penetrance and gender bias, with a marked male prevalence. Based on the different hormonal metabolism between genders, we proposed that estrogens play a protective role in females and showed that these hormones ameliorate mitochondrial dysfunction in LHON through the estrogen receptors (ERs). We also showed that ERβ localize to the mitochondria of RGCs. Thus, targeting ERβ may become a therapeutic strategy for LHON specifically aimed at avoiding or delaying the onset of disease in mutation carriers. Here, we tested the effects of ERβ targeting on LHON mitochondrial defective metabolism by treating LHON cybrid cells carrying the m.11778G>A mutation with a combination of natural estrogen-like compounds that bind ERβ with high selectivity. We demonstrated that these molecules improve cell viability by reducing apoptosis, inducing mitochondrial biogenesis and strongly reducing the levels of reactive oxygen species in LHON cells. These effects were abolished in cells with ERβ knockdown by silencing receptor expression or by using specific receptor antagonists. Our observations support the hypothesis that estrogen-like molecules may be useful in LHON prophylactic therapy. This is particularly important for lifelong disease prevention in unaffected LHON mutation carriers. Current strategies attempting to combat degeneration of RGCs during the acute phase of LHON have not been very effective. Implementing a different and preemptive approach with a low risk profile may be very helpful.

Received: August 19, 2015. **Revised and Accepted:** September 17, 2015

Introduction

Leber's Hereditary Optic Neuropathy (LHON [MIM 535000]) is a maternally inherited disease characterized by a subacute selective degeneration of retinal ganglion cells (RCGs) leading to optic nerve atrophy and loss of central vision, mostly in young men. LHON is almost always owing to one of three frequent pathogenic point mutations of mitochondrial DNA (mtDNA), affecting the complex I subunits genes *MT-ND4* (m.11778G>A), *MT-ND1* (m.3460G>A) and *MT-ND6* (m.14484T>C) (1). With an estimated frequency of ~1 in 50 000 in Europe (2,3,4,5), LHON represents one of the most common mitochondrial disorders and its treatment is an unmet clinical need. In fact, although the administration of antioxidants such as idebenone and EPI-743 showed encouraging results in promoting partial recovery of visual function (6,7,8,9), optic atrophy and permanent blindness still remain the usual outcomes of LHON. Peculiar features of LHON are incomplete penetrance and significant gender bias. LHON pathogenic mutations are usually homoplasmic (all mitochondrial DNA molecules are mutated), yet only ~50% of male and 10% of female mutation carriers lose vision (10,11). Investigations have revealed at least four modulators of LHON penetrance: the anatomical variation of the optic nerve head size leading to the 'crowded disc' as a risk factor (12), mtDNA background haplotypes increasing penetrance (13,14), ill-defined nuclear DNA background modifiers (15,16,17) and environmental factors such as tobacco smoking acting as disease triggers (18,19).

More recently, stemming from the male prevalence, we proposed that estrogens play a protective role in females by mitigating the deleterious effect of LHON mutations on mitochondrial functions (20). By using *trans*mitochondrial cybrids (herein cybrids), we demonstrated that 17β-estradiol (E2) reduces reactive oxygen species (ROS) production and ameliorates cell energetic competence by inducing mitochondrial biogenesis. These findings fit our *ex vivo* and *in vitro* studies showing that unaffected mutation carriers (i.e. individuals carrying the mutation that have not developed the disease after 35 years of age) display the most efficient compensatory mitochondrial biogenesis, as compared with controls and LHON affected individuals (21). Altogether, our observations provide an explanatory framework for incomplete penetrance with male prevalence in LHON and point to the crucial role played by the genetic and hormonal modulation of mitochondrial biogenesis.

Interestingly, the positive effects of estrogens are mediated by estrogen receptors (ERs), and ERβ, but not the ERα subtype, localizes to mitochondria of RGCs (20). Thus, targeting ERβ may be an effective therapeutic strategy for young unaffected carriers of the LHON mutation, to specifically avoiding or delaying the onset of disease. The option to target the ERβ pathway for therapeutic purposes is more attractive and safer than nonspecific targeting involving also ERα. This is because ERα, but not ERβ, activation mediates the undesirable side effects such as gynecomastia and decreased libido in men and elevated risk for breast and endometrial cancers in women (22). Furthermore, signaling through ERβ has been shown to play a major role in estrogen-mediated neuroprotection, myelination and promotion of neural synaptic plasticity (23,24,25). Accordingly, in the last few years, a mounting number of studies have shown the efficacy of ERβ-selective agonists in experimental models of neurodegenerative disease and other disorders, including autoimmune diseases, endometriosis, depression, hypertension and cancer (for a review, see 26). Presently, natural and synthetic ERβ agonists are being studied in human cancer, schizophrenia and metabolic syndrome (www.clinicaltrials.gov).

In the present work, we tested the effects of ERβ targeting on LHON mitochondrial defective metabolism by treating LHON cybrids carrying the m.11778G>A mutation with a combination of natural estrogen-like compounds (i.e. phytoestrogens genistein, G; daidzein, D and equol, Eq). This formulation was previously shown to bind ERβ with high selectivity, leading to a higher efficacy/safety profile as compared with single or other combined formulations (27). We here demonstrate that the phytoestrogens formulation improved cell viability by reducing apoptosis, inducing mitochondrial biogenesis and sharply reducing ROS levels in LHON cybrids. Most of these effects were abolished by ERβ knockdown.

Results

Phytoestrogens ameliorate LHON cell viability in galactose medium by reducing apoptosis

LHON cybrids growth in galactose medium display reduced viability as compared with controls because of apoptotic death (28,29). As we previously demonstrated, supplementation of medium with E2 rescued this pathological phenotype (20). We here show that incubation of LHON cells with a combination of the phytoestrogens G, D and Eq (each at 100 nM) increased viability (up to 70% as compared with vehicle) after 48 h incubation in galactose medium and decreased the rate of apoptosis (up to 50%) after 24 h. These results were comparable with those obtained with 100-nM E2 (Fig. 1A and B). The phytoestrogen treatment did not affect viability of control cells in galactose medium (Supplementary Material, Fig. S1A). Furthermore, supplementation with either E2 or single phytoestrogens did not impact cell growth rate of mutant or control cybrids in glucose medium (Supplementary Material, Fig. S1B). Interestingly, the rescue in viability of LHON cells was significantly milder when the phytoestrogens G, D or Eq were added alone at 100 nM (Supplementary Material, Fig. S1C). This last observation is in agreement with previous results by Zhao *et al.* (2009) showing that, when used in combination, the phytoestrogens G, D and Eq result in an overall improved efficacy as compared with the isolated compounds used at the same concentration (27). In addition, to verify that the better effect of the G+D+Eq combination was not merely due to an overall increased concentration of the estrogen-like molecules, we evaluated the effects of 300 nM of G, D and Eq alone on cells viability and showed no significant effect as compared with vehicle in this setting (Supplementary Material, Fig. S1D).

ERβ knockdown abolishes the effect of phytoestrogens on cell viability

To verify whether the effect of the G+D+Eq formulation on LHON cell viability was mediated by ERβ, we used two different approaches. First, we performed a transient silencing of the two ER isoforms by using specific siRNAs. As shown in Figure 1C, ERβ silencing (ERβ-) completely abolished the rescue effect of the G+D+Eq combination after 24 h incubation in galactose medium, whereas ERα silencing (ERα-) did not. The efficiency of silencing was evaluated by western blot analysis (Fig. 1D).

The second approach involved the use of selective pharmacologic antagonists of the two ER isoforms. Again, pre-incubation of LHON cybrids with 100 nM of the selective ERβ antagonist PHTPP abolished the effect of the G+D+Eq combination. In contrast, the inhibition of ERα by the MPP dihydrochloride (MPP) antagonist had no effect (Fig. 1E).

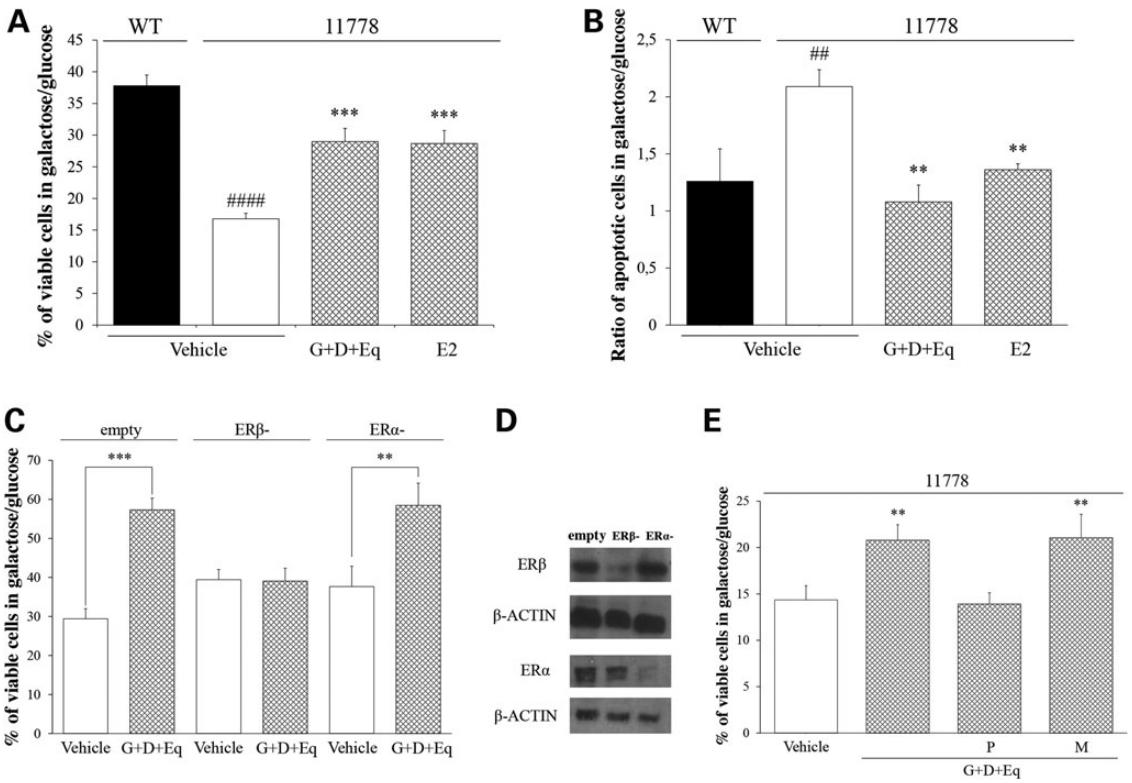

Figure 1. Viability of LHON cybrids treated with 17β-estradiol or with a phytoestrogens formulation. (**A**) Viability of control (WT) and LHON cybrids (11778) evaluated after 48 h of incubation in galactose medium supplemented with either 100 nM 17β-estradiol (E2), a combination of G+D+Eq (100 nM each) or vehicle. The number of viable cells in galactose is normalized to the number of viable cells in glucose at the same time point. Data are the mean ± SEM of four experiments in duplicate on two mutants and two control cybrids clones. (**B**) Apoptotic cell death of WT and LHON cybrids after 24 h of incubation in galactose medium supplemented with either 100 nM 17β-estradiol (E2), a combination of G+D+Eq (100 nM each) or vehicle. Data are expressed as a ratio between the percentage of apoptotic cells in galactose and in glucose medium. Data are mean ± SEM of three experiments on two mutants and two control cybrid clones. $^{\#\#}P < 0.01$; $^{\#\#\#\#}P < 0.0001$ for 11778 vehicle versus WT vehicle (*T*-student). $^{**}P < 0.01$; $^{***}P < 0.001$ for 11778 treated versus 11778 vehicle (ANOVA test). (**C**) Viability of LHON cybrids transiently transfected with either a specific siRNA against ERβ (ERβ-negative clones, ERβ-) or ERα (ERα-negative clones, ERα-). An empty siRNA was used as a negative control (empty). Viability was evaluated after 24 h of incubation in galactose medium ± G+D+Eq (100 nM each) or vehicle. The number of viable cells in galactose was normalized for the number of viable cells in glucose at the same time point. Data are mean ± SEM of three experiments in duplicate on two cybrid clones. $^{**}P < 0.01$, $^{***}P < 0.001$ for treated versus vehicle (*T*-student). (**D**) Representative western blot on transiently transfected cybrids showing significant reduction of ERβ but not ERα protein in ERβ-negative clones and significant reduction of ERα but not ERβ protein in ERα-negative clones. The β-actin protein was used as housekeeping. (**E**) Viability of LHON cybrids in the presence of either the selective ERβ antagonist PHTPP (P) or the selective ERα antagonist MPP (M) added 30 min before G+D+Eq to the medium. The number of viable cells in galactose medium was normalized for the number of viable cells in glucose medium after 48 h. Data are mean ± SEM of three experiments in duplicate on two clones. $^{**}P < 0.01$ for 11778 treated versus 11778 vehicle (ANOVA test).

The phytoestrogen formulation induces mitochondrial biogenesis through ERβ activation

In previous work, we showed that LHON mutation carriers display a more efficient mitochondrial biogenesis as compared with controls. This feature is more evident in unaffected carriers as compared with affected individuals, pointing to compensatory mitochondrial biogenesis as a modulator of disease penetrance (21). We have also shown that the beneficial effect of estrogens on LHON cell metabolism is largely mediated by the induction of mitochondrial biogenesis (20). Thus, we analyzed markers of mitochondrial biogenesis and mitochondrial density in LHON and control cells treated with the phytoestrogens formulation.

As shown in Figure 2A, after 24 h incubation in glucose medium supplemented with G+D+Eq (100 nM each), we observed a significant and coordinated induction (up to 2.5-fold increase) of the regulators of mitochondrial biogenesis *SIRT1*, *PGC1α* and *NRF1*. The key components of mitochondrial transcription and replication machinery *TFAM* and *POLG*, and the nuclear- and mitochondrial-encoded respiratory chain subunits *MTND6*, *NDUFA9*, *MTCOI* and *COIV* were also upregulated. Gene induction was more evident in LHON as compared with controls and was fully inhibited when cells were pre-incubated with the ERβ antagonist PHTPP. In contrast, when the ERα antagonist was added to the medium the induction of mitochondrial biogenesis was still evident, although to a lesser degree (Fig. 2A). We then evaluated the expression level of proteins belonging to different mitochondrial compartments (matrix, inner and outer mitochondrial membrane) showing a general upregulation in treated cells, more evident in LHON (Fig. 2B and C).

The upregulation of mitochondrial proteins was associated with an increase in mitochondrial density, as evaluated by ultrastructure and morphometric analysis and expressed both as the number of mitochondria per 100 μm^2 and as a mitochondrial/cytoplasmic area ratio (Fig. 3B). As shown in Figure 3A, treatment with phytoestrogens did not impact on mitochondrial size and shape.

Induction of mitochondrial biogenesis leads to increased respiratory competence of LHON cybrids

To assess whether induction of mitochondrial biogenesis reflects into improved mitochondrial energetics, we evaluated the respiration

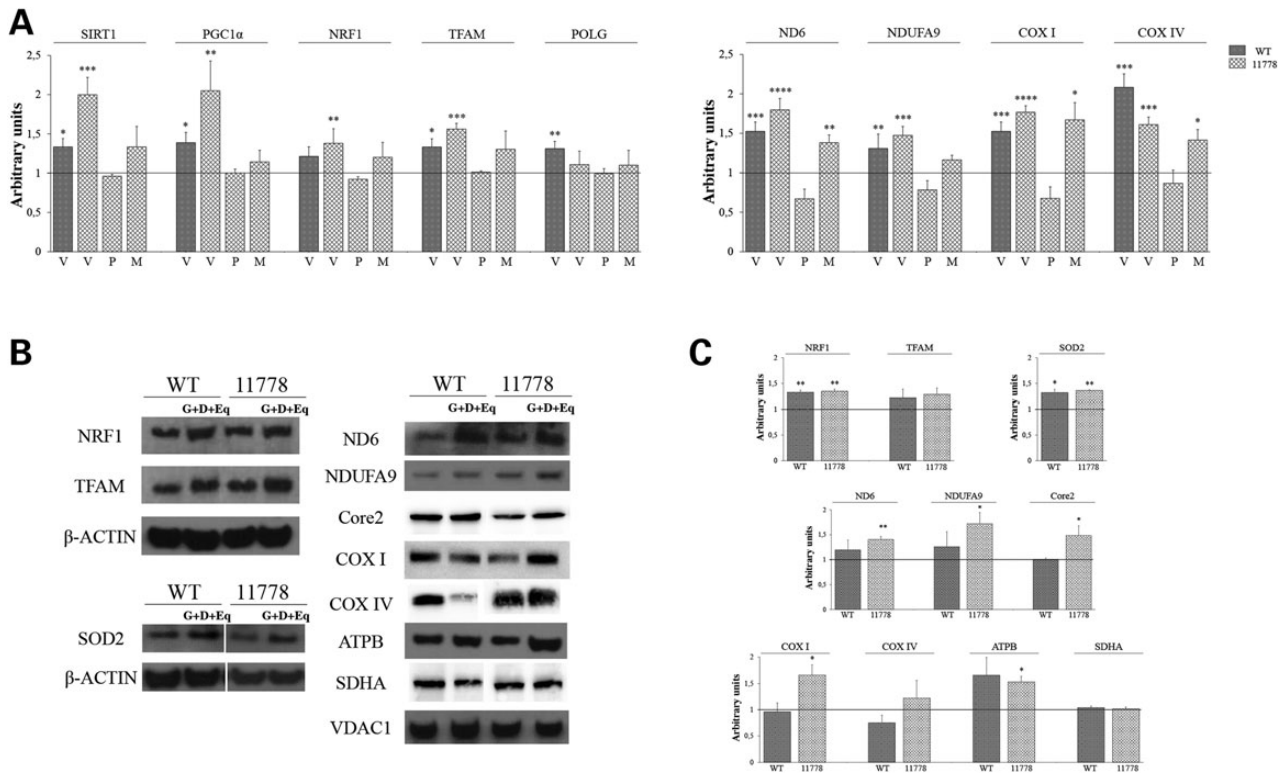

Figure 2. Evaluation of mitochondrial biogenesis in control and LHON cybrids treated with the phytoestrogen formulation. (**A**) The relative mRNA expression of the master regulators of mitochondrial biogenesis (*SIRT1*, *PGC1* and *NRF1*), the key components of the mitochondrial transcription and replication machinery (*TFAM* and *POLG*) and the nuclear- and mitochondrial-encoded respiratory chain subunits (*ND6*, *NDUFA9*, *COX I* and *COX IV*) were evaluated by real-time PCR analysis on control (WT) and LHON (11778) cells incubated 24 h in glucose medium supplemented with G+D+Eq (100 nM each) or with vehicle (V). In a subset of experiments, LHON cybrids were pre-incubated with 100 nM of either the selective ERβ antagonist PHTPP (P) or the selective ERα antagonist MPP (M). Data are expressed as treated/vehicle ratio and are mean ± SEM of three experiments in duplicate on two mutant and two cybrid clones. $^{*}P < 0.05$, $^{**}P < 0.01$, $^{***}P < 0.001$ for treated cells versus vehicle (*T*-student) (dark gray = WT; light gray = LHON) (**B** and **C**). Protein expression evaluated on control and LHON cells incubated 24 h in glucose medium supplemented with G+D+Eq or vehicle (V): representative western blot and densitometry are shown (mean ± SEM). Protein level was expressed as treated/vehicle ratio. Experiments were performed at least in duplicate for all samples. $^{*}P < 0.05$, $^{**}P < 0.01$ for treated cells versus vehicle (*T*-student).

capability of mutant and control cybrids by using both the Clark-type electrode and the microscale oxygraphy. As expected, we observed reduced oxygen consumption in LHON as compared with controls. Treatment with the G+D+Eq formulation led to a significant increase in both basal oxygen consumption rate (up to 2-fold in LHON) and maximal respiration capacity after 24 h (Fig. 3C and D).

To further characterize the energetic competence of cybrid cells, we measured the ATP synthesis driven by CI (pyruvate/malate) and CII (succinate) substrates in cells incubated for 24 h in glucose medium with or without the G+D+Eq combination. Again, as expected, we measured a reduced ATP synthesis driven by CI substrates in LHON cybrids compared with controls. In these conditions of maximal phosphorylation, we failed to appreciate any differences between treated and untreated cells (Supplementary Material, Fig. S2) supporting the hypothesis that estrogen mainly acts by inducing an overall increase in mitochondrial biogenesis.

The phytoestrogen formulation decreases oxidative stress in cybrid cells

There is previous evidence that production of mitochondrial ROS is significantly increased in LHON cybrids (30,31) and supplementation with E2 significantly reduced superoxide (O_2^-) levels (20). Thus, we investigated mitochondrial O_2^- levels in treated and untreated cells using the MitoSOX™ Red fluorescence probe. We showed that LHON cybrids presented higher O_2^- levels as compared with controls in basal condition (glucose medium). Levels increased further when LHON cells were incubated 1 h in galactose medium. Supplementation with phytoestrogens dramatically reduced O_2^- levels both in glucose and galactose (Fig. 4A). We confirmed, by flow cytometry, a significantly higher (up to 1.3-fold) production of O_2^- in LHON as compared with controls. Again supplementation with the G+D+Eq formulation substantially rescued this pathologic phenotype (Fig. 4A). The reduction of O_2^- was paralleled, within 1 h, by the activation of the mitochondrial isoform of superoxide dismutase (SOD), the Manganese (Mn) SOD (Fig. 4B). Finally, we measured H_2O_2 levels by a luminescent assay. In basal conditions, LHON cybrids showed higher amounts of H_2O_2 levels (up to 2-fold increase) as compared with controls, and again, phytoestrogen treatment led to a 1.2-fold decrease (Fig. 4C).

The beneficial effects of phytoestrogens also occurred in cells from patients in the context of their nuclear background

All the results presented were obtained in cybrids, a cell model that evaluates the effect of mtDNA mutations in a neutral nuclear background (i.e. osteosarcoma cell line). Since we showed that a different nuclear background between affected and

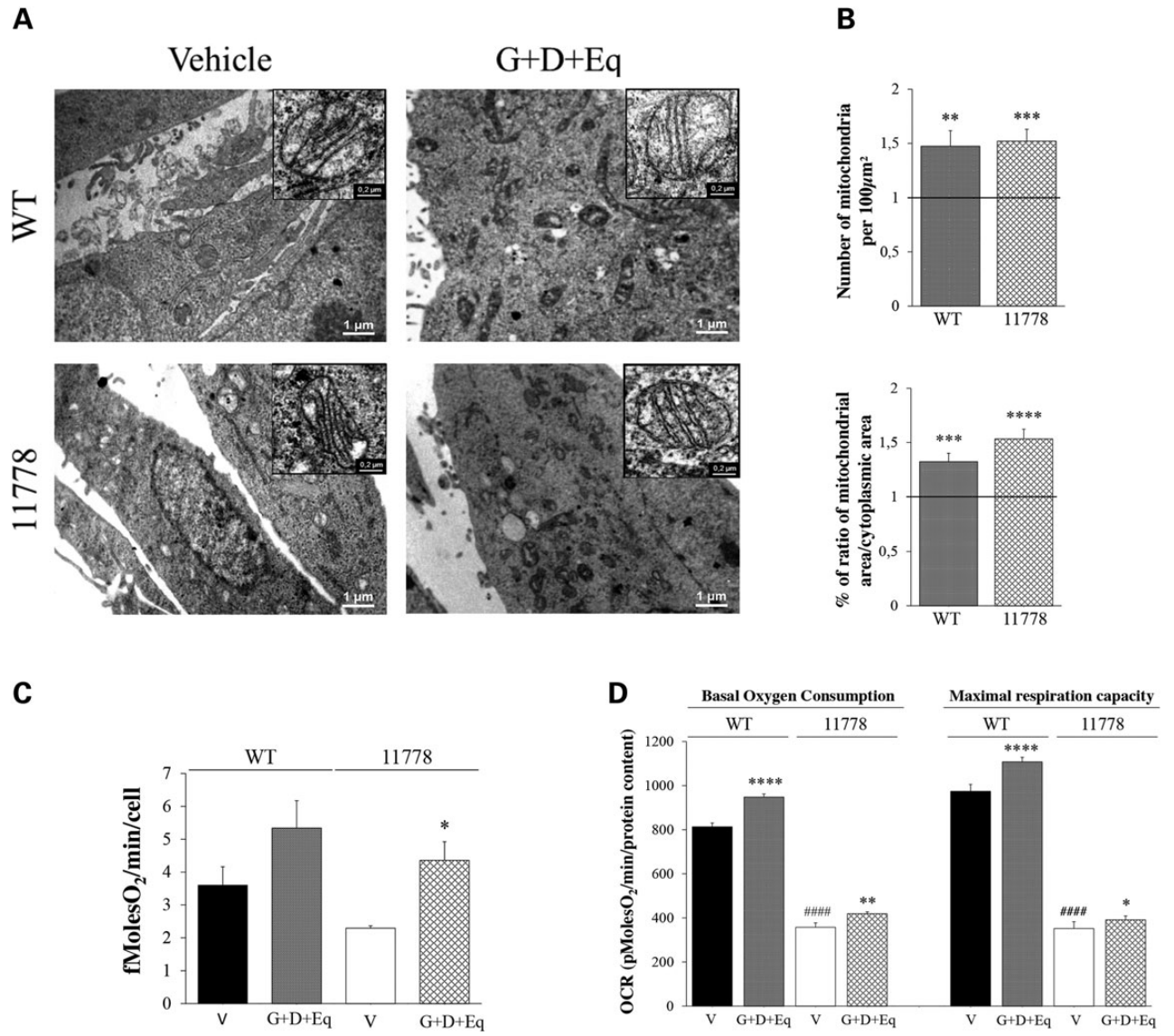

Figure 3. The phytoestrogens formulation increases mitochondrial density and ameliorates the bioenergetics competence of the cells. (**A**) Representative ultrastructural images of control (WT) and LHON (11778) cybrids incubated 24 h in glucose medium supplemented with G+D+Eq (100 nM each) or vehicle. Inserts represent higher magnification images showing mitochondrial cristae. (**B**) For each condition, 15 random fields at 8000× magnification were acquired and the number of mitochondria per 100 μm^2 (upper panel) and mitochondrial/cytoplasmic area ratio (bottom panel) were obtained by using ImageJ 64 1.48v. Data are expressed as treated/vehicle ratio and are mean ± SEM of two experiments on two control and two mutant cybrid clones. $^{**}P < 0.01$, $^{***}P < 0.001$, $^{****}P < 0.0001$ for treated cells versus vehicle (*T*-student). (**C**) Rate of oxygen consumption in control (WT) and LHON (11778) cells treated with G+D+Eq (100 nM each) or vehicle for 24 h. Data are mean ± SEM of two experiments on two control and two mutant cybrid clones. $^{*}P < 0.05$ for treated cells versus vehicle (*T*-student). (**D**) OCR values were obtained in WT and LHON cybrids at resting conditions (basal oxygen consumption) and in the presence of 1 µM FCCP (maximal respiratory capacity) after 24-h incubation in glucose medium supplemented with G+D+Eq (100 nM each) or vehicle. Data are mean ± SEM of at least three independent experiments. $^{\#\#\#\#}P < 0.0001$ for 11778 vehicle versus WT vehicle (*T*-student). $^{*}P < 0.05$, $^{**}P < 0.01$, $^{****}P < 0.0001$ for treated cells versus vehicle (*T*-student).

unaffected LHON carriers modulates the penetrance of the mtDNA mutation (21), we evaluated the effect of phytoestrogens on fibroblasts derived from affected and unaffected mutation carriers and controls.

We confirmed that in galactose medium fibroblasts from controls and unaffected LHON carriers grew at a similar rate, whereas fibroblasts from affected individuals grew at a significantly slower rate (21). This pathologic phenotype was completely rescued by supplementation of medium with the G+D+Eq formulation. Phytoestrogens had no significant effect on the growth rate of controls and unaffected carriers (Fig. 5B).

As expected, we found that ERβ localized to the nucleus and co-localized with the mitochondrial network of fibroblasts (Supplementary Material, Fig. S3).

Discussion

A formulation of phytoestrogens consisting of G+D+Eq led to the rescue of mitochondrial dysfunction in LHON cybrids, at a similar magnitude as using E2. Multiple pathways with different timings may possibly drive this rescue. The earliest effect of phytoestrogens is probably on oxidative stress, as exemplified by an increase

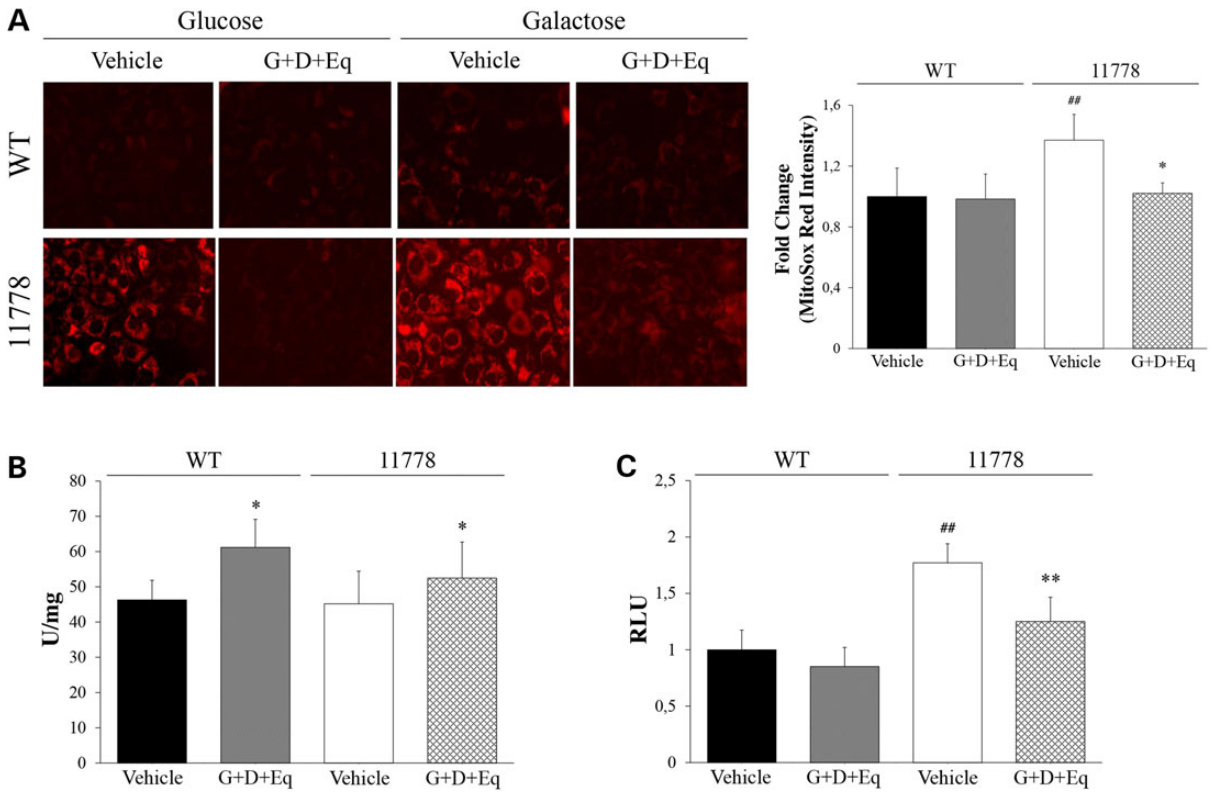

Figure 4. Evaluation of oxidative stress in control and LHON cybrids treated with phytoestrogens formulation. (**A**) Mitochondrial superoxide levels (O_{2-}) were evaluated in treated and untreated cells using the MitoSOX™ Red probe. For immunofluorescence staining, cells were maintained for 1 h in glucose or galactose medium ± G+D+Eq (100 nM each), then incubated with MitoSOX™ Red for 15 min, washed and observed under an Olympus IX50 Fluorescence microscope. Representative images of two experiments on two mutant and two control cybrid clones are shown. O_{2-} levels were quantified by flow cytometry after 1 h of incubation in glucose medium ± G+D +Eq. Data are mean ± SEM of two experiments on two control and two mutant cell lines. $^{\#\#}P < 0.01$ for 11778 vehicle versus WT vehicle (*T*-student). $^{*}P < 0.05$ for 11778 treated versus 11778 vehicle (*T*-student). (**B**) Mitochondrial MnSOD activity was evaluated in treated and untreated cells as described in Materials and Methods and expressed as units/mg protein. Data are mean ± SEM of eight experiments on two control and two mutant cell lines. $^{*}P < 0.05$ for treated versus vehicle (*T*-student). (**C**) Cells were maintained 2 h in glucose medium ± G+D+Eq, and then H_2O_2 levels were evaluated by luminescent assay using the ROS-Glo™ H_2O_2 assay. Data are mean ± SEM of two experiments on two control and two mutant cybrid clones. $^{\#\#}P < 0.01$ for 11778 vehicle versus WT vehicle (*T*-student). $^{*}P < 0.05$ for 11778 treated versus 11778 vehicle (*T*-student).

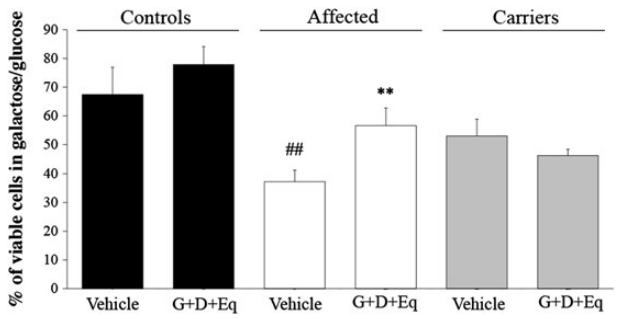

Figure 5. Viability of LHON fibroblasts treated with phytoestrogens. Viability was evaluated after 72 h of incubation in galactose medium supplemented with G+D +Eq (100 nM each) or vehicle. The number of viable cells in galactose was normalized to the number of viable cells in glucose at the same time point. Data are the mean ± SEM of two experiments in duplicate on three affected, three unaffected carriers and three control cell lines. $^{\#\#}P < 0.01$ for 11778 vehicle versus WT vehicle (*T*-student), $^{**}P < 0.01$ for treated cells versus vehicle (*T*-student).

in MnSOD activity and a decrease of O_2^- and H_2O_2, within the first hour of cell treatment. At later times, but within 24 h, we observed the phytoestrogen-dependent activation of mitochondrial biogenesis, which in turn leads to increased cell respiration. Most importantly, the whole metabolic compensation is specifically promoted by the ERβ and not by ERα, making possible the avoidance of serious side effects that would restrict the use of E2 *in vivo*. The proof of principle that we obtained in LHON cybrid cells was also seen in the patient-derived fibroblasts. Given our previous demonstration that ERβ is expressed in RGCs (20), there seems to be great promise in therapy using this approach to mitigate the neurodegeneration seen in LHON. We propose that this approach could be of therapeutic value particularly to maintain the neuroprotection of RGCs in unaffected mutation carriers to preclude their conversion to vision loss and optic atrophy.

In our study, we looked at the two relevant pathogenic mechanisms induced by complex I dysfunction in LHON: impaired bioenergetics and increased oxidative stress. Both can predispose to cell death by apoptosis and thus hamper cell viability, as previously shown in the LHON cybrid cell model (28,31,32,33). Concerning bioenergetics, the phytoestrogen treatment improved respiration by activating mitochondrial biogenesis and increasing mitochondrial density. This is similar to what we described for E2 (20) and probably occurs naturally as means for the successful compensatory response in adult unaffected individuals carrying the mutation (21). In our experimental model, the results also clearly demonstrate the dependence of phytoestrogen effects on mitochondrial biogenesis from ERβ, and not from ERα. Furthermore, we also confirm the occurrence of increased oxidative stress in LHON cybrids, and we have been able to rescue cells

from this pathologic mechanism by phytoestrogen treatment. However, distinct from the mechanisms on mitochondrial bioenergetics, the phytoestrogen effect on oxidative stress is acute, the rescue becoming apparent within the very first hour after treatment. We interpret this as a direct effect of phytoestrogens on MnSOD, as shown by our and others previous studies (20,34,35,36).

The key point in using phytoestrogens as a therapeutic strategy remains that ERβ largely mediate the compensatory effects on LHON cells, avoiding the potentially harmful effects on cell proliferation and sexual differentiation. Thus, this approach could be feasible in patients promoting a rapid translation into clinical practice. Accordingly, the neuroprotective potential of molecules targeting the ERβ is currently a hot topic of many pharmacology research programs (26). An issue for molecules to be used at best advantage in eye pathology would be the ideal of topical administration, as recently investigated with some promising results in glaucoma (37). Bioavailability to the disease target, the RGCs, needs to be explored keeping in mind the difficulties with drug diffusion across the vitreous to the retina.

LHON is characterized by a subacute, rapidly evolving neurodegeneration leading to RGC death, probably by apoptosis and without major inflammatory changes. To date, medical treatments for the acute phase of LOHN have not been truly effective even in the clinical studies with the quinones, idebenone and EPI-743 (6,7,8,9). At best these studies showed a better final outcome of treated patients by increasing the rate of visual recovery, possibly limiting axonal loss, without stopping the disease progression in most cases. We envisage phytoestrogens as a preventive approach specifically for individuals who are non-symptomatic carriers of the LHON mutation who always remain at risk of converting. The early and sustained treatment of LHON patients has better promise to modify the natural history in preserving RGCs from cell death. Thus, we propose the use of phytoestrogens primarily for unaffected mutation carriers, in particular those who present with subclinical changes such as nerve fiber layer swelling and microangiopathic features (38).

As shown by our studies, the therapeutic strategy based on E2 and phytoestrogens impinges on the same, naturally occurring, compensatory mechanism we recently reported as central for LHON penetrance, the activation of mitochondrial biogenesis (20,21). In fact, on the low pathogenic potential of LHON mutations, ultimately leading to a reduced complex I-driven ATP synthesis rate, an increased mitochondrial density may overcome the bioenergetic defect inducing an overall increase in the total ATP levels, as we previously shown (20), and boosting respiration. Thus, females may be protected by hormonal modulation (20), whereas for both genders, there is also an unknown genetically determined background driving the efficiency in activating mitochondrial biogenesis (21). In addition, our results reveal how phytoestrogens rapidly buffer the high levels of oxidative stress in LHON cells. This antioxidant effect is even more important than the correction of bioenergetics, as recently corroborated by the results from the LHON mouse model with ND6 mtDNA mutation, where the primary pathogenic mechanism was related to oxidative stress overproduction, and not to ATP deficiency (39).

In conclusion, the current study provides evidence that phytoestrogen can correct *in vitro* the cellular pathologic phenotype associated with LHON mutations, in both cybrids and patient-derived fibroblasts. The natural origin of phytoestrogens makes these molecules more suited for a rapid translation into clinical trials, given that synthetic ERβ compounds are not yet validated for clinical use. The target population for the phytoestrogen therapy may be the large pool of unaffected mutation carriers within LHON maternal lineages, who are at high risk of conversion and might benefit from preventive therapy, to avoid vision loss for the rest of their lives. We would encourage, as a next step, a trial with these phytoestrogens in the LHON genetic mouse model.

Materials and Methods

Cell lines and reagents

Fibroblast primary cultures were established from skin biopsies from three affected and three unaffected mutation carriers (bearing the homoplasmic m.11778G>A mutation), and from three normal donors.

Osteosarcoma-derived (143B.TK-) cybrid cell lines were selected from a previously established collection to match mtDNA haplogroup between LHON and controls and were as follows: LHON cybrids bearing the m.11778G>A mutation (HPE9, haplogroup J1c; HFF3, haplogroup U5a) and controls (HGA, haplogroup J1c; HGdA8, haplogroup U1). All the cybrid clones were previously characterized, and the complete mitochondrial DNA sequence had been determined (40,41,42).

Fibroblasts and cybrids were grown in high glucose DMEM (Life Technologies, Warrington, UK) supplemented with dialyzed fetal bovine serum (15% for fibroblasts and 10% for cybrids) (Life Technologies), 110 mg/ml sodium pyruvate, 2 mM L-glutamine, 100 U/ml penicillin and 100 mg/ml streptomycin (Life Technologies) (referred to as glucose medium) in a humidified atmosphere of 95% air and 5% CO_2 at 37°C. Experiments were performed both in glucose medium and in glucose-free DMEM, supplemented with dialyzed fetal bovine serum, 5 mM galactose (Sigma–Aldrich St Louis, MO, USA) and 110 mg/ml sodium pyruvate (Life Technologies) (referred to as galactose medium).

17β-estradiol (E2), genistein (G), daidzein (D) and equol (Eq) were purchased from Sigma–Aldrich; the ERβ antagonist PHTPP and the ERα antagonist MPP were purchased from Tocris Bioscience (Bristol, UK). E2 was dissolved in ethanol. The phytoestrogens G, D, Eq and the antagonist MPP and PHTPP were dissolved in DMSO.

Cell viability

Cell growth was measured by the Trypan blue dye exclusion assay. Multiple series of 30 mm of diameter (for fibroblasts) and 60 mm of diameter (for cybrids) dishes were seeded with a constant number of cells (either 2 or 3×10^5). Cells were growth either in glucose or galactose medium (a condition forcing cells to rely on oxidative metabolism for ATP synthesis) for 24, 48 and 72 h with the addition of one of the following: E2, G, D and Eq (each at concentrations of either 100 or 300 nM); or a combination of G plus D plus Eq (each at 100 nM). In a subset of experiments, 100 nM of either PHTPP or MPP were added 30 min before the incubation of phytoestrogens. Untreated cells were maintained at the same final ethanol/DMSO concentration. Cells were harvested with 0.25% trypsin and 0.2% EDTA, washed, suspended in PBS in the presence of Trypan blue solution (Sigma–Aldrich) at 1:1 ratio and counted using a hemocytometer. For each time point, the number of viable cells in galactose medium was expressed as a percentage of the number of cells in glucose.

Rate of apoptosis by flow cytometer

To test the rate of apoptosis, treated and untreated cells were seeded at $0.5–1 \times 10^6$ in glucose or galactose medium for 24 h.

Cells were washed and harvested in Binding Buffer 1× (BD Biosciences, Franklin Lakes, NJ, USA) by scraping to minimize potentially high annexin V background levels in adherent cells. Cells were stained with APC-conjugated annexin V (BD Biosciences) and analyzed on a FACS-Calibur flow cytometer (BD Biosciences) (43).

Small interfering RNA (siRNA) transfection

A number of 4×10^5 cells were seeded in 60 mm of diameter dishes and maintained in glucose medium for 24 h. Then, cells were transfected with 60 pmol of siRNA specific for ERβ or ERα (ESR2, ESR1; Life Technologies) using Lipofectamine™ RNAi^{MAX} Transfection Reagent (Life Technologies) according to the manufacturer's protocol. After 24 h, cells were harvested and seeded at 3×10^5 in glucose or galactose medium plus or minus the combination of G+D+Eq and to evaluate cell viability. Transfection efficiency was evaluated by western blot analysis.

Oxygen consumption

Oxygen consumption rate (OCR) in adherent cells was measured with an XFe24 Extracellular Flux Analyzer (Seahorse Bioscience, Billerica, MA, USA), as previously described (44,45), with minor variations. Briefly, cells were seeded in XFe24 cell culture microplates at 8×10^3 cells/well in 250 µl of glucose medium and incubated at 37°C in 5% CO_2 for 24 h. The day after, the medium was replaced with fresh glucose medium containing vehicle or a combination of G plus D plus Eq (each at 100 nM), and cells were incubated for further 24 h. Assays were initiated following the manufacturer's instructions by replacing the growth medium in each well with 525 µl of unbuffered DMEM-high glucose prewarmed at 37°C. Cells were incubated at 37°C for 60 min to allow temperature and pH equilibration. After an OCR baseline measurement, 75 µl of medium containing oligomycin, FCCP, rotenone and antimycin A were sequentially added to each well to reach final concentrations of 1 µM oligomycin, 0.2 µM FCCP, and 1 µM rotenone and antimycin A. At the end of experiment, cell content for each well was determined using the colorimetric sulforhodamine B assay, as previously detailed (46). Data are expressed as picomoles of O_2 per minute per protein content.

As a second approach, we also measured oxygen consumption in treated and untreated intact cells ($2\text{-}3 \times 10^6$) using a Clark-type oxygen electrode (Hansatech, Norfolk, UK) in 1 ml DMEM lacking glucose and supplemented with 10% sodium pyruvate, as described previously (47).

Mitochondrial ATP synthesis

The rate of mitochondrial ATP synthesis was measured in digitonin-permeabilized cells by using the luciferin/luciferase assay, according to the Materials and Methods previously described (48), with minor modifications (44). Briefly, after trypsinization, cells (10×10^6/ml) were suspended in a buffer containing 150 mM KCl, 25 mM Tris–HCl, 2 mM EDTA, 0.1% bovine serum albumin, 10 mM potassium phosphate, 0.1 mM MgCl2, pH 7.4, kept at room temperature for 15 min, then incubated with 50 µg/ml digitonin until 90–100% of cells were positive to Eritrosine B staining. Aliquots of 3×10^5 permeabilized cells were incubated in the same buffer in the presence of the adenylate kinase inhibitor P^1, P^5-di(adenosine-5′) pentaphosphate (0.1 mM), and the CI substrates (1 mM malate plus 1 mM pyruvate) or the CII substrate (5 mM succinate plus 2 µg/ml rotenone). After addition of 0.1 mM ADP, chemiluminescence was determined as a function of time with a luminometer. The chemiluminescence signal was calibrated with an internal ATP standard after addition of 10 µM oligomycin. The rates of ATP synthesis were normalized to protein contents (49) and citrate synthase activity (50). Each value was the mean based on at least four independent determinations.

Gene expression by quantitative real-time polymerase chain reaction

Total RNA was isolated from treated and untreated cells using SV Total RNA isolation kit (Promega, Fitchburg, WI, USA) and measured with a NanoDrop ND-1000 spectrophotometer (NanoDrop Technologies, Wilmington, DE, USA). Total RNA (0.1–1 mg) was reverse-transcribed to cDNA using random hexamer primers. The relative expression levels of *SIRT1*, *PPARGC1A* (alias *PGC1-α*), *NRF1, TFAM, POLG, MT-ND6, NDUAF9, MT-COI, COIV, ESR1* and *ESR2* genes were evaluated. We used TaqMan probe chemistry by means of inventoried FAM-labeled TaqMan® MGB probes (Life Technologies), according to the manufacturer's instructions (Supplementary Material, Table S1). In all samples, the relative expression of each target gene was evaluated with respect to one control (reference sample) using the comparative threshold cycle (ΔCt) method. All values were normalized HPRT1 housekeeping genes.

Western blot analysis

Treated and untreated cells were rinsed twice with ice-cold PBS, lysed in ice-cold RIPA buffer (50 mM Tris–HCl pH 8, 150 mM NaCl, 1% NP-40, 0.5% sodium deoxycholate, 1% sodium dodecyl sulfate, 1 mM phenylmethylsulfonyl fluoride, 10 mg/ml aprotinin, 10 mg/ml leupeptin and 10 mg/ml pepstatin) and centrifuged at 10000*g* for 10 min at 4°C. For a set of experiments, mitochondria were isolated from cybrid cells by standard differential centrifugation.

Protein concentration was measured by bicinchoninic acid (Beyotime Biotechnology, Haimen, China). Equal amount of protein (40 µg) was separated by precast 4–20% BoltTM Mini Gels (Life Technologies) and transferred to a polyvinylidene fluoride membrane. Primary antibodies were visualized using horseradish peroxidase-conjugated secondary antibodies (Dako, Glostrup, Denmark). Signals were detected by enhanced chemiluminescence (Amersham Biosciences, UK).

The following primary antibodies were used: mouse monoclonal antibody anti-β-actin (Sigma–Aldrich); rabbit polyclonal antibody anti-ERα; rabbit polyclonal antibody anti-ERβ; goat polyclonal antibody anti-TFAM; rabbit polyclonal antibody anti-NRF1 (Santa Cruz Biotech, Santa Cruz, CA, USA); rabbit polyclonal antibody anti-SOD2; rabbit polyclonal antibody anti-ND6; mouse monoclonal antibody anti-NDUFA9; mouse monoclonal antibody anti-SDHA; mouse monoclonal antibody anti-COXI; mouse monoclonal antibody anti-COXIV; mouse monoclonal antibody anti-CORE2; mouse monoclonal antibody anti-ATPB; mouse monoclonal antibody anti-VDAC1/Porin (Abcam, Cambridge, UK).

Densitometry was performed using ImageJ64 1.48 v (National Institute of Health, Bethesda, MD, USA).

Reactive oxygen species evaluation

Mitochondrial superoxide (O_2^-) level was evaluated in treated and untreated cells using a mitochondrial ROS indicator MitoSOX™ Red (Invitrogen Molecular Probes, Life Technologies). Once in the mitochondria, MitoSOX™ reagent is oxidized by superoxide and exhibits a red fluorescence (with excitation at

510 nm and emission at 580 nm). For live imaging experiment, cells were maintained in glucose medium for 1 h, washed with Hank's Buffered Salt Solution 1× (HBSS) containing calcium and magnesium and then incubated with 5 μM MitoSOX™ reagent for 15 min in the dark at 37°C. After removing MitoSOX™, cells were washed with HBSS 1× and fluorescent images were acquired with an Olympus IX50 Fluorescence microscope. For flow cytometry, cells were maintained in glucose medium for 1 h, washed with PBS and treated with 5 μM MitoSOX™ reagent for 30 min in the dark at 37°C. Then, cells were washed with PBS, collected by centrifugation, suspended in Binding Buffer 1× (BD Biosciences) and immediately analyzed with FACS-Calibur flow cytometer (BD Biosciences).

Levels of hydrogen peroxide (H_2O_2) were measured by luminescence assay using a ROS-Glo™ H_2O_2 Assay (Promega) according to the manufacturer's protocol. A number of 1×10^4 cells were plated in a 96-well white cell culture plate and incubated overnight in 100 μl of glucose medium. Then, medium was replaced by 80 μl of fresh glucose medium plus or minus phytoestrogens, supplemented with 20 μl of H_2O_2 Substrate Dilution Buffer containing 125 μM ROS-Glo™ H_2O_2. After 2-h incubation, 100 μl of ROS-Glo™ Detection Solution was added and the plate was incubated for 20 min at room temperature. Luminescence was determined with a GloMax® Multi+ Luminometer. The average RLU of triplicate samples were calculated.

MnSOD activity was performed as follows. After 1-h incubation in glucose medium containing a combination of G plus D plus Eq (each at 100 nM), cells were harvested from a 75-cm^2 flask, resuspended to 10×10^6/ml in 0.25 M Sucrose, 10 mM Tris and 0.2 mM EDTA pH 7.6. Then, cells were permeabilized with 100 μg/ml digitonin for 1 min at room temperature and centrifuged at 10000*g* for 5 min at 4°C. The pellet of cells enriched in mitochondria was resuspended in 0.125 mM Tris, 0.1% Triton X-100 and 2 mM KCN pH 7.8. The suspension was immediately used for MnSOD evaluation, using a Superoxide Dismutase Assay kit (Sigma–Aldrich) following the manufacturer's protocol. The assay kit is designed to measure total SOD activity, but the presence of KCN in the buffer inhibits both cytosolic Cu/Zn-SOD and extracellular SOD, resulting largely in the detection of MnSOD activity alone.

Ultrastructural and histomorphometric analysis

Treated and untreated cells were initially fixed adding in room temperature 2.5% glutaraldehyde to culture medium in a 1:1 ratio. The culture/fixative mix was transferred into plastic vials and centrifuged at 10 000*g* for 10 min at room temperature to generate a cell pellet. Supernatant was removed, and pellets were rinsed with PBS buffer, after which final fixation was obtained storing the pellets with 2.5% glutaraldehyde overnight at 4°C followed by 1 h of osmium tetroxide fixation.

Tissue dehydration, resin embedding and staining were performed as described (51). Grids were observed with an FEI Morgagni 268 TEM (FEI Corporate, Hillsboro, OR, USA) and 15 random fields at 8000× magnification were acquired and stored as TIFF images (Digital Micrograph 3.4TM, Gatan. GMBH, Munchen, Germany). Image analysis was performed using ImageJ 64 1.48v (GNU License, National Institute of Health). Mitochondria were counted, the perimeter of each organelle was manually traced and the mitochondrial area was automatically measured. Both the total and the mean cross-sectional mitochondrial area were then obtained for each acquired field. The cytoplasmic area was also manually measured for each image, and the ratio between total mitochondrial area and cytoplasmic area was then derived.

To explore mitochondrial 'cristae', high-power magnification images were acquired from each group and stored as TIFF images.

Statistical analysis

All data are expressed as mean ± SEM. Data were analyzed by standard ANOVA procedures followed by multiple pair-wise comparison adjusted with Bonferroni corrections. Chi-square test was used for frequency data. Significance was considered at $P < 0.05$. Numerical estimates were obtained with the GraphPad InStat 3 version (GraphPad, Inc., San Diego, CA, USA).

Supplementary Material

Supplementary Material is available at *HMG* online.

Acknowledgements

We thank Dr Maurizia Orlandi and Dr Massimiliano Mancini for their excellent technical assistance.

Conflict of Interest statement. None declared.

Funding

This work was supported by the United Mitochondrial Disease Foundation, grant 12-059 (to C.G.), MITOCON ONLUS, and by Associazione Serena Talarico per i giovani nel mondo. Partial support has also been provided by Telethon-Italy, grant #GGP14187 (to V.C.).

References

1. Newman, N.J. (2005) Hereditary optic neuropathies. In: Miller, N.R., Newman, N.J., Biousse, V. and Kerrison, J.B. (eds), *Walsh & Hoyt's Clinical Neuro Ophthalmology*. Philadelphia: Lippincott Williams & Williams. pp. 465–501.
2. Man, P.Y.W., Griffiths, P.G., Brown, D.T., Howell, N., Turnbull, D.M. and Chinnery, P.F. (2003) The epidemiology of Leber hereditary optic neuropathy in the North East of England. *Am. J. Hum. Genet.*, **72**, 333–339.
3. Spruijt, L., Kolbach, D.N., de Coo, R.F., Plomp, A.S., Bauer, N.J., Smeets, H.J. and de Die-Smulders, C.E. (2006) Influence of mutation type on clinical expression of Leber hereditary optic neuropathy. *Am. J. Ophthalmol.*, **141**, 676–682.
4. Puomila, A., Hämäläinen, P., Kivioja, S., Savontaus, M.L., Koivumäki, S., Huoponen, K. and Nikoskelainen, E. (2007) Epidemiology and penetrance of Leber hereditary optic neuropathy in Finland. *Eur. J. Hum. Genet.*, **15**, 1079–1089.
5. Mascialino, B., Leinonen, M. and Meier, T. (2012) Meta-analysis of the prevalence of Leber hereditary optic neuropathy mtDNA mutations in Europe. *Eur. J. Ophthalmol.*, **22**, 461–465.
6. Klopstock, T., Yu-Wai-Man, P., Dimitriadis, K., Rouleau, J., Heck, S., Bailie, M., Atawan, A., Chattopadhyay, S., Schubert, M., Rummey, C. *et al.* (2011) A randomized placebo-controlled trial of idebenone in Leber's hereditary optic neuropathy. *Brain*, **134**, 2677–2686.
7. Carelli, V., La Morgia, C., Valentino, M.L., Rizzo, G., Carbonelli, M., De Negri, A.M., Sadun, F., Carta, A., Guerriero, S., Simonelli, F. *et al.* (2011) Idebenone treatment in Leber's hereditary optic neuropathy. *Brain*, **134**, e188.
8. Klopstock, T., Metz, G., Yu-Wai-Man, P., Büchner, B., Gallenmüller, C., Bailie, M., Nwali, N., Griffiths, P.G., von Livonius, B., Reznicek, L. *et al.* (2013) Persistence of the treatment effect

of idebenone in Leber's hereditary optic neuropathy. *Brain*, **136**, e230.
9. Sadun, A.A., Chicani, C.F., Ross-Cisneros, F.N., Barboni, P., Thoolen, M., Shrader, W.D., Kubis, K., Carelli, V. and Miller, G. (2012) Effect of EPI-743 on the clinical course of the mitochondrial disease Leber hereditary optic neuropathy. *Arch. Neurol.*, **69**, 331–338.
10. Carelli, V., Ross-Cisneros, F.N. and Sadun, A.A. (2004) Mitochondrial dysfunction as a cause of optic neuropathies. *Prog. Retin. Eye Res.*, **23**, 53–89.
11. Man, P.Y., Griffiths, P.G., Hudson, G. and Chinnery, P.F. (2009) Inherited mitochondrial optic neuropathies. *J. Med. Genet.*, **46**, 145–158.
12. Ramos, C.V., Bellusci, C., Savini, G., Carbonelli, M., Berezovsky, A., Tamaki, C., Cinoto, R., Sacai, P.Y., Moraes-Filo, M.N., Miura, H.M. *et al.* (2009) Association of optic disc size with development and prognosis of Leber's hereditary optic neuropathy. *Invest. Ophthalmol. Vis. Sci.*, **50**, 1666–1674.
13. Carelli, V., Achilli, A., Valentino, M.L., Rengo, C., Semino, O., Pala, M., Olivieri, A., Mattiazzi, M., Pallotti, F., Carrara, F. *et al.* (2006) Haplogroup effects and recombination of mitochondrial DNA: novel clues from the analysis of Leber hereditary optic neuropathy pedigrees. *Am. J. Hum. Genet.*, **78**, 564–574.
14. Hudson, G., Carelli, V., Spruijt, L., Gerards, M., Mowbray, C., Achilli, A., Pyle, A., Elson, J., Howell, N., La Morgia, C. *et al.* (2007) Clinical expression of Leber hereditary optic neuropathy is affected by the mitochondrial DNA-haplogroup background. *Am. J. Hum. Genet.*, **81**, 228–233.
15. Hudson, G., Keers, S., Yu Wai Man, P., Griffiths, P., Huoponen, K., Savontaus, M.L., Nikoskelainen, E., Zeviani, M., Carrara, F., Horvath, R. *et al.* (2005) Identification of an X-chromosomal locus and haplotype modulating the phenotype of a mitochondrial DNA disorder. *Am. J. Hum. Genet.*, **77**, 1086–1091.
16. Shankar, S.P., Fingert, J.H., Carelli, V., Valentino, M.L., King, T. M., Daiger, S.P., Salomao, S.R., Berezovsky, A., Belfort, R. Jr., Braun, T.A. *et al.* (2008) Evidence for a novel x-linked modifier locus for leber hereditary optic neuropathy. *Ophthalmic. Genet.*, **29**, 17–24.
17. Ji, Y., Jia, X., Li, S., Xiao, X., Guo, X. and Zhang, Q. (2010) Evaluation of the X-linked modifier loci for Leber hereditary optic neuropathy with the G11778A mutation in Chinese. *Mol. Vis.*, **16**, 416–424.
18. Sadun, A.A., Carelli, V., Salomao, S.R., Berezovsk, A., Quiros, P. A., Sadun, F., De Negri, A.M., Andrade, R., Moraes, M., Passos, A. *et al.* (2003) Extensive investigation of a large Brazilian pedigree of 11778/haplogroup J Leber hereditary optic neuropathy. *Am. J. Ophthalmol.*, **136**, 231–238.
19. Kirkman, M.A., Yu-Wai-Man, P., Korsten, A., Leonhardt, M., Dimitriadis, K., De Coo, I.F., Klopstock, T., Chinnery, P.F., Sadun, F., DeNegri, A.M. *et al.* (2009) Gene-environment interactions in Leber hereditary optic neuropathy. *Brain*, **132**, 2317–2326.
20. Giordano, C., Montopoli, M., Perli, E., Orlandi, M., Fantin, M., Ross-Cisneros, F.N., Caparrotta, L., Martinuzzi, A., Ragazzi, E., Ghelli, A. *et al.* (2011) Oestrogens ameliorate mitochondrial dysfunction in Leber's hereditary optic neuropathy. *Brain*, **134**, 220–234.
21. Giordano, C., Iommarini, L., Giordano, L., Maresca, A., Pisano, A., Valentino, M.L., Caporali, L., Liguori, R., Deceglie, S., Roberti, M. *et al.* (2014) Efficient mitochondrial biogenesis drives incomplete penetrance in Leber's hereditary optic neuropathy. *Brain*, **137**, 335–353.
22. Deroo, B.J. and Korach, K.S. (2006) Estrogen receptors and human disease. *J. Clin. Invest.*, **116**, 561–570.
23. Rissman, E.F., Heck, A.L., Leonard, J.E., Shupnik, M.A. and Gustafsson, J.A. (2002) Disruption of estrogen receptor β gene impairs spatial learning in female mice. *Proc. Natl Acad. Sci. USA*, **99**, 3996–4001.
24. Liu, F., Day, M., Muñiz, L.C., Bitran, D., Arias, R., Revilla-Sanchez, R., Grauer, S., Zhang, G., Kelley, C., Pulito, V. *et al.* (2008) Activation of estrogen receptor-beta regulates hippocampal synaptic plasticity and improves memory. *Nat. Neurosci.*, **11**, 334–343.
25. Khalaj, A.J., Yoon, J., Nakai, J., Winchester, Z., Moore, S.M., Yoo, T., Martinez-Torres, L., Kumar, S., Itoh, N. and Tiwari-Woodruff, S.K. (2013) Estrogen receptor (ER) β expression in oligodendrocytes is required for attenuation of clinical disease by an ERβ ligand. *Proc. Natl Acad. Sci. USA*, **110**, 19125–19130.
26. Nilsson, S., Koehler, K.F. and Gustafsson, J.Å. (2011) Development of subtype-selective oestrogen receptor-based therapeutics. *Nat. Rev. Drug. Discov.*, **10**, 778–792.
27. Zhao, L., Mao, Z. and Brinton, R.D. (2009) A select combination of clinically relevant phytoestrogens enhances estrogen receptor beta-binding selectivity and neuroprotective activities in vitro and in vivo. *Endocrinology*, **150**, 770–783.
28. Ghelli, A., Zanna, C., Porcelli, A.M., Schapira, A.H., Martinuzzi, A., Carelli, V. and Rugolo, M. (2003) Leber's hereditary optic neuropathy (LHON) pathogenic mutations induce mitochondrial-dependent apoptotic death in transmitochondrial cells incubated with galactose medium. *J. Biol. Chem.*, **278**, 4145–4150.
29. Zanna, C., Ghelli, A., Porcelli, A.M., Martinuzzi, A., Carelli, V. and Rugolo, M. (2005) Caspase-independent death of Leber's hereditary optic neuropathy cybrids is driven by energetic failure and mediated by AIF and Endonuclease G. *Apoptosis*, **10**, 997–1007.
30. Beretta, S., Mattavelli, L., Sala, G., Tremolizzo, L., Schapira, A. H., Martinuzzi, A., Carelli, V. and Ferrarese, C. (2004) Leber hereditary optic neuropathy mtDNA mutations disrupt glutamate transport in cybrid cell lines. *Brain*, **127**, 2183–2192.
31. Floreani, M., Napoli, E., Martinuzzi, A., Pantano, G., De Riva, V., Trevisan, R., Bisetto, E., Valente, L., Carelli, V. and Dabbeni-Sala, F. (2005) Antioxidant defences in cybrids harboring mtDNA mutations associated with Leber's hereditary optic neuropathy. *FEBS J.*, **272**, 1124–1135.
32. Vergani, L., Martinuzzi, A., Carelli, V., Cortelli, P., Montagna, P., Schievano, G., Carrozzo, R., Angelini, C. and Lugaresi, E. (1995) MtDNA mutations associated with Leber's hereditary optic neuropathy: studies on cytoplasmic hybrid (cybrid) cells. *Biochem. Biophys. Res. Commun.*, **210**, 880–888.
33. Baracca, A., Solaini, G., Sgarbi, G., Lenaz, G., Baruzzi, A., Schapira, A.H., Martinuzzi, A. and Carelli, V. (2005) Severe impairment of complex I-driven adenosine triphosphate synthesis in leber hereditary optic neuropathy cybrids. *Arch. Neurol.*, **62**, 730–736.
34. Borrás, C., Gambini, J., Gómez-Cabrera, M.C., Sastre, J., Pallardó, F.V., Mann, G.E. and Viña, J. (2005) 17beta-oestradiol upregulates longevity-related antioxidant enzyme expression via the ERK1 and ERK2[MAPK]/NFkappaB cascade. *Aging Cell*, **4**, 113–118.
35. Pedram, A., Razandi, M., Wallace, D.C. and Levin, E.R. (2006) Functional estrogen receptors in the mitochondria of breast cancer cells. *Mol. Biol. Cell.*, **17**, 2125–2137.
36. Gottipati, S. and Cammarata, P.R. (2008) Mitochondrial superoxide dismutase activation with 17 beta-estradiol-treated human lens epithelial cells. *Mol. Vis.*, **14**, 898–905.
37. Prokai-Tatrai, K., Xin, H., Nguyen, V., Szarka, S., Blazics, B., Prokai, L. and Koulen, P. (2013) 17β-estradiol eye drops protect

the retinal ganglion cell layer and preserve visual function in an in vivo model of glaucoma. *Mol. Pharm.*, **10**, 3253–3261.
38. Barboni, P., Savini, G., Feuer, W.J., Budenz, D.L., Carbonelli, M., Chicani, F., Ramos, C.D., Salomao, S.R., De Negri, A., Parisi, V. *et al.* (2012) Retinal nerve fiber layer thickness variability in Leber hereditary optic neuropathy carriers. *Eur. J. Ophthalmol.*, **22**, 985–991.
39. Lin, C.S., Sharpley, M.S., Fan, W., Waymire, K.G., Sadun, A.A., Carelli, V., Ross-Cisneros, F.N., Baciu, P., Sung, E., McManus, M. J. *et al.* (2012) Mouse mtDNA mutant model of Leber hereditary optic neuropathy. *Proc. Natl Acad. Sci. USA*, **109**, 20065–20070.
40. Pello, R., Martín, M.A., Carelli, V., Nijtmans, L.G., Achilli, A., Pala, M., Torroni, A., Gómez-Durán, A., Ruiz-Pesini, E., Martinuzzi, A. *et al.* (2008) Mitochondrial DNA background modulates the assembly kinetics of OXPHOS complexes in a cellular model of mitochondrial disease. *Hum. Mol. Genet.*, **17**, 4001–4011.
41. Ghelli, A., Porcelli, A.M., Zanna, C., Vidoni, S., Mattioli, S., Barbieri, A., Iommarini, L., Pala, M., Achilli, A., Torroni, A. *et al.* (2009) The background of mitochondrial DNA haplogroup J increases the sensitivity of Leber's hereditary optic neuropathy cells to 2,5-hexanedione toxicity. *PLoS One*, **4**, e7922.
42. Perli, E., Giordano, C., Tuppen, H.A., Montopoli, M., Montanari, A., Orlandi, M., Pisano, A., Catanzaro, D., Caparrotta, L., Musumeci, B. *et al.* (2012) Isoleucyl-tRNA synthetase levels modulate the penetrance of a homoplasmic m.4277T>C mitochondrial tRNA(Ile) mutation causing hypertrophic cardiomyopathy. *Hum. Mol. Genet.*, **21**, 85–100.
43. Campese, A.F., Grazioli, P., Colantoni, S., Anastasi, E., Mecarozzi, M., Checquolo, S., De Luca, G., Bellavia, D., Frati, L., Gulino, A. *et al.* (2009) Notch3 and pTalpha/pre-TCR sustain the in vivo function of naturally occurring regulatory T cells. *Int. Immunol.*, **21**, 727–743.
44. Giorgio, V., Petronilli, V., Ghelli, A., Carelli, V., Rugolo, M., Lenaz, G. and Bernardi, P. (2012) The effects of idebenone on mitochondrial bioenergetics. *Biochim. Biophys. Acta*, **1817**, 363–369.
45. Iommarini, L., Kurelac, I., Capristo, M., Calvaruso, M.A., Giorgio, V., Bergamini, C., Ghelli, A., Nanni, P., De Giovanni, C., Carelli, V. *et al.* (2014) Different mtDNA mutations modify tumor progression in dependence of the degree of respiratory complex I impairment. *Hum. Mol. Genet.*, **23**, 1453–1466.
46. Porcelli, A.M., Ghelli, A., Iommarini, L., Mariani, E., Hoque, M., Zanna, C., Gasparre, G. and Rugolo, M. (2008) The antioxidant function of Bcl-2 preserves cytoskeletal stability of cells with defective respiratory complex I. *Cell. Mol. Life Sci.*, **65**, 2943–2951.
47. Carelli, V., Vergani, L., Bernazzi, B., Zampieron, C., Bucchi, L., Valentino, M., Rengo, C., Torroni, A. and Martinuzzi, A. (2002) Respiratory function in cybrid cell lines carrying European mtDNA haplogroups: implications for Leber's hereditary optic neuropathy. *Biochim. Biophys. Acta*, **1588**, 7–14.
48. Manfredi, G., Yang, L., Gajewski, C.D. and Mattiazzi, M. (2002) Measurements of ATP in mammalian cells. *Methods*, **26**, 317–326.
49. Bradford, M.M. (1976) A rapid and sensitive method for the quantitation of microgram quantities of protein utilizing the principle of protein-dye binding. *Anal. Biochem.*, **72**, 248–254.
50. Trounce, A., Kim, Y.L., Jun, A.S. and Wallace, D.C. (1996) Assessment of mitochondrial oxidative phosphorylation in patient muscle biopsies, lymphoblasts, and transmitochondrial cell lines. *Methods Enzymol.*, **264**, 484–509.
51. Mascorro, J.A. and Bozzola, J.J. (2007) Processing biological tissues for ultrastructural study. *Methods Mol. Biol.*, **369**, 19–34.